RESEARCH PAPER

A novel electrochemical DNA biosensor construction based on layered CuS–graphene composite and Au nanoparticles

**Chun-Xuan Xu · Qiu-Ge Zhai · Yu-Jie Liu ·
Ke-Jing Huang · Lu Lu · Ke-Xin Li**

Abstract A novel CuS–graphene (CuS-Gr) composite was synthesized to achieve excellent electrochemical properties for application as a DNA electrochemical biosensor. CuS-Gr composite was prepared by a hydrothermal method, in which two-dimensional graphene served as a two-dimensional conductive skeleton to support CuS nanoparticles. A sensitive electrochemical DNA biosensor was fabricated by immobilizing single-stranded DNA (ss-DNA) labeled at the 5′ end using 6-mercapto-1-hexane (HS-ssDNA) on the surface of Au nanoparticles (AuNPs) to form ssDNA-S–AuNPs/CuS-Gr, and hybridization sensing was done in phosphate buffer. Cyclic voltammetry and electrochemical impedance spectroscopy were performed for the characterization of the modified electrodes. Differential pulse voltammetry was applied to monitor the DNA hybridization using an $[Fe(CN)_6]^{3-/4-}$ solution as a probe. Under optimum conditions, the biosensor developed exhibited a good linear relationship between the current and the logarithm of the target DNA concentration ranging from 0.001 to 1 nM, with a low detection limit of 0.1 pM ($3\sigma/S$). The biosensor exhibited high selectivity to differentiate one-base-mismatched DNA and three-base-mismatched DNA. The results indicated that the sensing platform based on CuS-Gr provides a stable and conductive interface for electrochemical detection of DNA hybridization, and could easily be extended to the detection of other nucleic acids.

Keywords CuS–graphene composite · Gold nanoparticles · DNA biosensor · DNA hybridization

C.-X. Xu · Q.-G. Zhai · Y.-J. Liu · K.-J. Huang (✉) · L. Lu ·
K.-X. Li
College of Chemistry and Chemical Engineering, Xinyang Normal University, Xinyang 464000, Henan, China
e-mail: kejinghuang@163.com

K.-J. Huang
State Key Laboratory of Chemo/Biosensing and Chemometrics,
College of Chemistry and Chemical Engineering, Hunan University,
Changsha 410082, Hunan, China

Introduction

DNA detection is highly important in some areas related to human health, such as diagnosis of infectious diseases, genetic mutations, and clinical medicines [1, 2]. DNA biosensors provide a powerful means of recognizing specific DNA sequences, and different biosensors have been reported for detection of specific DNA sequences [3–5]. Among them, electrochemical DNA biosensors are attracting great interest with regard to simplification of the analysis, miniaturization, and microelectronic integration [6, 7].

Immobilization of DNA is a key step for construction of electrochemical DNA biosensors because it usually improves the stability of DNA and ensures intimate contact between the probe DNA and the target DNA. Nanomaterials have a large surface area and good conductivity, providing more binding sites and surface-enhanced charge transfer for enhanced selectivity and sensitivity. Therefore, various nanomaterials, such as graphene oxide (GO) [8], gold nanoparticles (AuNPs) [9], conducting polymers [10], carbon spheres [11], and carbon nanotubes [12], have been prepared for this purpose.

Graphene is a two-dimensional carbon nanomaterial and has been widely explored in the preparation of versatile devices such as field-effect transistors, electrochemical sensors, and microelectronic devices owing to the high mobility of charge carriers within it, its large specific surface area, the quantum Hall effect, and its outstanding electric conductivity [13–15], and therefore it was thought of as a robust atomic-

scale scaffold for nanoparticles to form hybrid materials with improved properties. Many studies have reported using graphene as a burgeoning support to disperse and stabilize metal, metal oxide, and semiconductor nanomaterials, such as Pt, ZnO, TiO$_2$, and ZnS, and these hybrid materials usually exhibit excellent catalytic, magnetic, or optoelectronic properties [16]. CuS is a p-type semiconductor and has been extensively applied in lithium rechargeable batteries, solar cells, biology markers, and biosensors because it is inexpensive, nontoxic, easily produced, and readily stored and has high specific capacitances [17–19]. However, it is not favorable for applications in electrode materials because of its low conductivity. Thus, it is highly desirable to prepare a CuS nanocomposite on an electronically conductive support to facilitate charge transfer for electrochemical biosensing applications. Therefore, the combination of graphene and CuS nanoparticles to prepare the nanocomposite would be a good way to improve the conductivity of CuS and the dispersibility of graphene nanosheets.

AuNPs are mostly recommended because they can greatly increase the current response of the modified sensor, because of their conductive ability and immobilization of biomolecules by a Au–S bond [20]. Recently, AuNPs have been extensively used in DNA hybridization sensing for amplification of hybridization owing to their catalytic properties, and they also exhibit high electrical and thermal conductivities [21, 22].

In this work, CuS–graphene (CuS-Gr) nanocomposite was synthesized by a hydrothermal method. A sensitive and label-free electrochemical biosensing strategy for detection of specific oligonucleotide sequences was then developed by assembling a DNA probe on CuS-Gr nanocomposite and an AuNP-modified electrode with a thiol-group-tagged DNA strand. After the target DNA had hybridized with the DNA probe to form a double-stranded structure on the biosensor surface, the electrochemical response of $[Fe(CN)_6]^{3-/4-}$ decreased, giving the quantitative foundation for target DNA detection. By integrating the CuS-Gr composite and AuNP signal amplification, the proposed strategy exhibited a low detection limit for the target DNA, with a wide linear range and good selectivity for base discrimination.

Experimental

Apparatus

Electrochemical measurements were performed with a CHI 660D electrochemical workstation (Shanghai CH Instruments, China) with a conventional three-electrode system composed of platinum wire as the auxiliary electrode, a saturated calomel electrode as the reference electrode, and a 3-mm-diameter glassy carbon electrode (GCE) as the working electrode. A JEM 2100 transmission electron microscope

(TEM) with an accelerating voltage of 200 kV and a Hitachi S-4800 scanning electron microscope (SEM) were used to record the morphologies of the nanocomposite. The X-ray powder diffraction pattern was obtained using a Rigaku D/Max-Ra x-ray diffractometer equipped with graphite monochromatized high-intensity Cu Kα radiation (λ=1.54178 Å) and operated at 40 kV and 20 mA. Raman spectra were recorded at ambient temperature using a Renishaw Raman system model 1000 spectrometer with a 200-mW argon-ion laser at an excitation wavelength of 514.5 nm and an integration time of 30 s.

Reagents

Graphite powder, hydrazine solution (50 wt%), ammonia solution (28 wt%), chloroauric acid (HAuCl$_4$·4H$_2$O), and trisodium citrate were purchased from Shanghai Chemical Reagent Corporation (Shanghai, China). The sulfhydryl-modified 18-base oligonucleotide probe [probe single-stranded DNA (ssDNA)], target complementary sequence DNA (target ssDNA), one-base-mismatched ssDNA, three-base-mismatched ssDNA, and noncomplementary sequence DNA (noncomplementary DNA) were synthesized by Shanghai Sangon Biological Engineering Technological Company (Shanghai, China). All DNA sequences were artificial sequences and were synthesized using standard phosphoramidite chemistry and purified using reversed-phase high-performance liquid chromatography. Their base sequences were as follows:

- Capture probe DNA (S1): 5′-SH-(CH$_2$)$_6$-TCT TTG GGA CCA CTG TCG-3′
- Complementary target to S1 (S2): 5′-CGA CAG TGG TCC CAA AGA-3′
- One-base-mismatched (underlined) target to S1 (S3): 5′-CGA CAG TGG TCC CAA C̲GA-3′
- Three-base-mismatched (underlined) target to S1 (S4): 5′-CGA CA̲A TGG C̲CC CAA C̲GA-3′
- Noncomplementary target to S1 (S5): 5′-GCA TCG AGC GAG CAC GTA-3′

All oligonucleotides were dissolved in 0.01 M phosphate buffer solution (PBS; pH 7.4) with 1 M NaCl and were kept frozen.

Synthesis of CuS-Gr composite

Firstly, GO was prepared by a modified Hummers method [23], and CuS was prepared according to a previous method [24]. The synthesis of CuS-Gr composite was performed as follows: 16 mg polyvinylpyrrolidone was firstly dissolved in 20 mL GO aqueous solution (0.1 mg mL^{-1}), and then 0.025 mmol CuCl$_2$ was added. The mixture was magnetically stirred at medium speed at room temperature to form a

homogeneous solution. Subsequently, 20 mL Na$_2$S (0.075 mmol) was added, and the mixture was stirred at slow speed at room temperature for 30 min. The mixture was then transferred to a 100-mL Teflon-lined stainless steel autoclave, the vessel containing the mixture was sealed tightly, and the mixture was heated at 180 °C for 24 h. After natural cooling to room temperature, the resulting suspension was centrifuged for 10 min at 12,000 rpm to remove unreacted GO in the supernatant and was washed with water three times to remove excess polyvinylpyrrolidone, Na$_2$S, and CuCl$_2$, and was dried at 50 °C for 12 h to obtain the CuS-Gr composite.

Preparation of the electrochemical DNA biosensor

CuS-Gr composite (1 mg) was dispersed in 1 mL water. The GCE (3-mm diameter) was polished with 1.0, 0.3, and 0.05 μm aluminum slurry to a mirrorlike surface to remove adsorbed organic matter, and was then sonicated in HNO$_3$, ethanol, and doubly distilled water, respectively. After drying in a nitrogen atmosphere, 10 μL CuS-Gr (1 mg mL^{-1}) suspension was applied onto the pretreated GCE surface and naturally dried in air to form the modified electrode, which was denoted as CuS-Gr/GCE. Subsequently, AuNPs were formed on the CuS-Gr/GCE by electrochemical deposition at -0.2 V for 80 s in 1.0 mM HAuCl$_4$ containing 0.1 M KCl to obtain the AuNPs/CuS-Gr/GCE. Immobilization of thiolated probe ssDNA (S1) was performed by directly dropping 10 μL S1 (1.0 μM) onto the surface of the AuNPs/CuS-Gr/GCE, followed by incubation at 25 °C for 12 h. The electrode obtained was denoted as S1/AuNPs/CuS-Gr/GCE. Then, the modified surface was washed with PBS (pH 7.0) to eliminate the nonspecifically adsorbed probe ssDNA molecules on the electrode surface. Then, the S1/AuNPs/CuS-Gr/GCE was subjected to 6-mercapto-1-hexane (1.0 mM) treatment for 1 h to further eliminate the nonspecifically adsorbed ssDNA molecules and to create a good orientation of the probe ssDNA for its good recognition ability. Then, 10 μL complementary target ssDNA sequence (S2) was applied on the S1/AuNPs/CuS-Gr/GCE for hybridization at 30 °C for 50 min. Finally, the electrode was washed with PBS to remove the unhybridized S2 and the hybridized electrode S2–S1/AuNPs/CuS-Gr/GCE was obtained. A schematic diagram of the stepwise procedure for the DNA biosensor fabrication is shown in Fig. 1.

Electrochemical detection

Cyclic voltammetry was performed in the potential range from -0.2 to 0.6 V at a scan rate of 100 mV s^{-1}. Differential pulse voltammetry (DPV) was performed in the scan range from -0.2 to 0.6 V, with a pulse amplitude of 50 mV, a pulse width of 50 ms, and a pulse period of 0.2 s. Electrochemical impedance spectroscopy was performed in a 10.0-mL aqueous solution containing 5 mM [Fe(CN)$_6$]$^{3-/4-}$ and 0.1 M KCl at a potential of 0.2 V over the frequency range from 0.1 Hz to 100 kHz, using an amplitude of 5 mV.

Results and discussion

Characterization of CuS-Gr composite

As shown in Fig. 2, an SEM and a TEM were used to characterize the morphologies of the as-prepared composites.

Fig. 1 The electrochemical DNA biosensor. *AuNP* gold nanoparticle, *cDNA* complementary DNA, *MCH* 6-mercapto-1-hexane
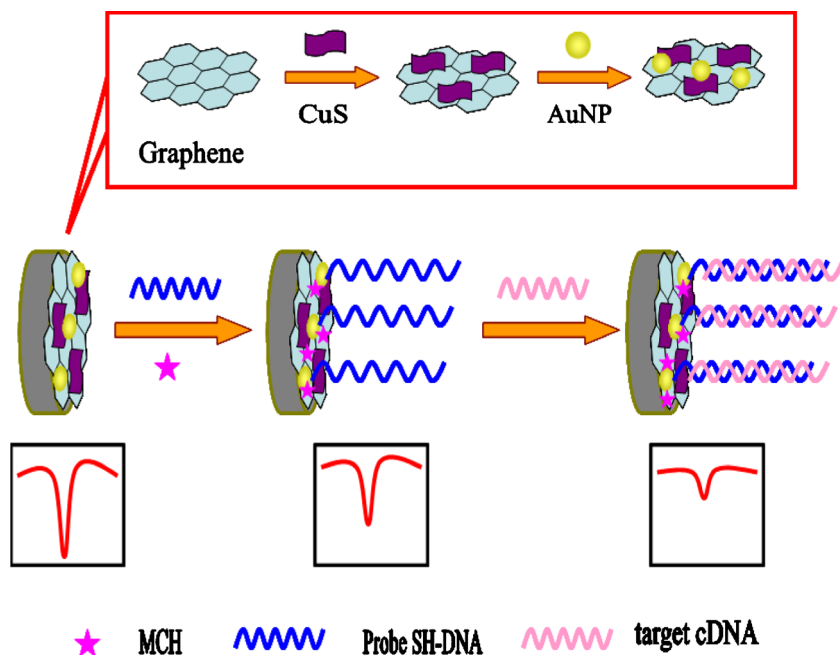
Fig. 2 Scanning electron
microscope images of graphene
oxide (GO) (**a**), CuS (**b**), and
CuS–graphene (CuS-Gr)
composite (**c**), and transmission
electron microscope images
of GO (**d**), CuS (**e**), CuS-Gr
composite (**f**), and graphene (**g**)
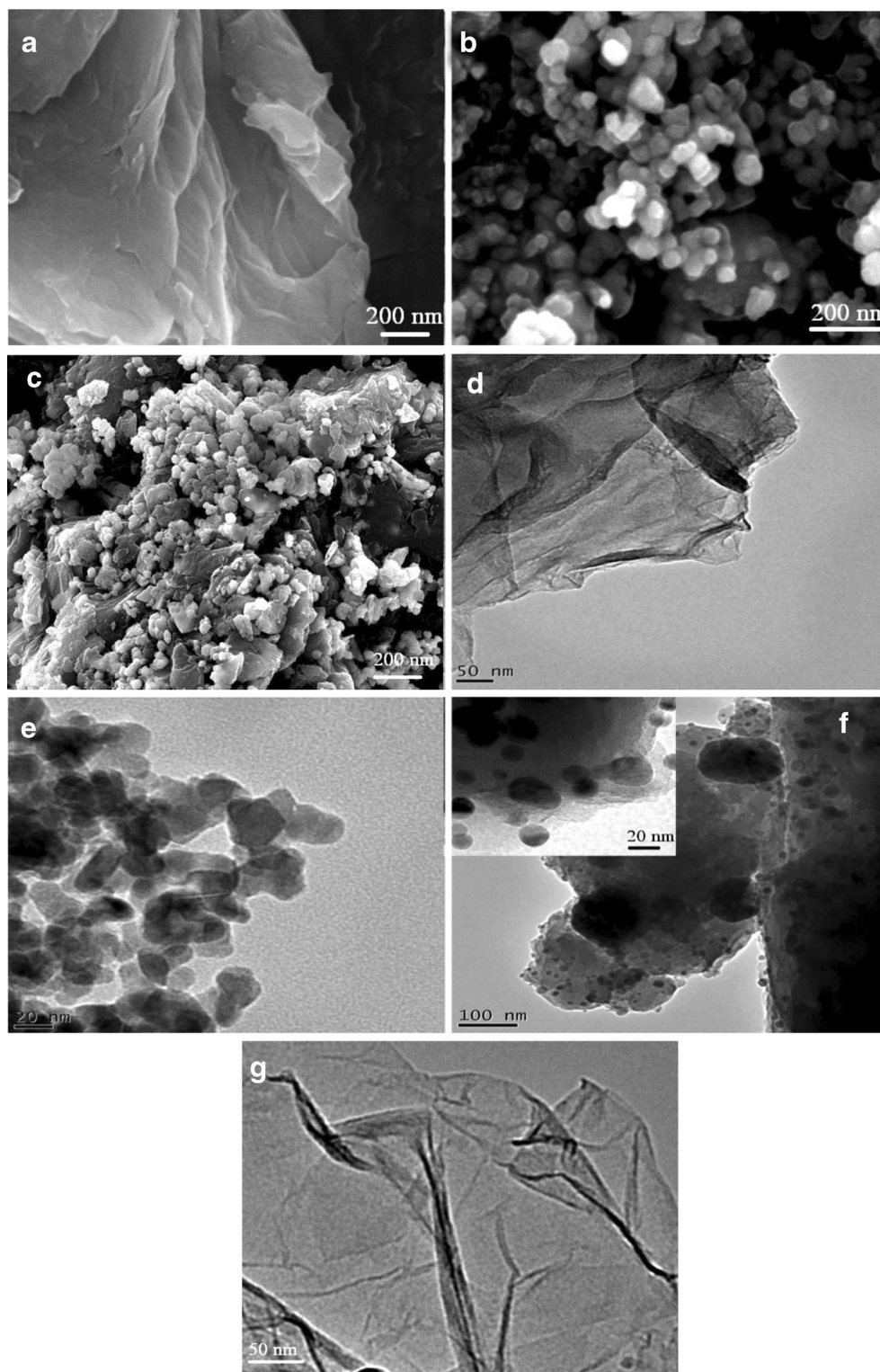
The SEM image in Fig. 2a reveals few-layer flexible wrinkled sheets of the GO. The SEM image of CuS shows CuS nanoparticles with uniform size (Fig. 2b). Figure 2c shows a representative SEM image of the synthesized CuS-Gr composite. A large number of CuS nanoparticles were well

dispersed on the surface of the graphene. The TEM image of GO shows the typical structure consisting of thin layers folded and tangled together (Fig. 2d). The TEM image in Fig. 2e confirms the results in Fig. 2b. As shown in Fig. 2f, CuS nanoparticles were well distributed on graphene nanosheets,
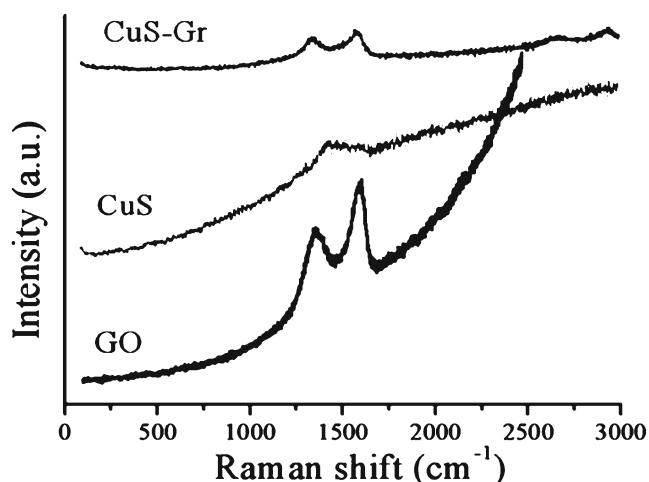
Fig. 3 Raman spectra of GO, CuS, and CuS-Gr composite

evidencing the well-behaved assembly process. The embedding of CuS on graphene nanosheets helps to prevent the aggregation of graphene. Furthermore, the surface functionalization with CuS nanoparticles can be a good way to improve the solubility and dispersibility of graphene nanosheets, and the unique properties of graphene nanosheets are maintained. Figure 2g shows a TEM image of graphene; it displays a typical crinkly and rippled structure.

The formation of CuS-Gr composite was also evidenced by the corresponding Raman spectra. Figure 3 shows the Raman spectra of GO, CuS, and CuS-Gr composite. It is clearly shows that two characteristic main peaks of GO, the D band at approximately 1,350 cm^{-1} and the G band at approximately 1,570 cm^{-1}, appear in the spectra of the GO and CuS-Gr samples. The 2D band at about 2,700 cm^{-1} that is characteristic of graphene is observed in CuS-Gr samples, which evidences that GO was successfully reduced to graphene.

Figure 4a shows the cyclic voltammograms of different modified electrodes obtained in a 1.0 mM $[Fe(CN)_6]^{3-/4-}$ solution containing 0.1 M KCl at a scan rate of 100 mV s^{-1}. The

bare GCE shows a well-defined reversible redox behavior of $[Fe(CN)_6]^{3-/4-}$ (curve a). After modification of the surface of the GCE with CuS-Gr composite, the redox peak currents increase greatly and the peak potential difference (ΔE_p) between the anodic and cathodic peaks decreases (curve b). After attachment of AuNPs on the CuS-Gr/GCE, an almost unchanged peak current of the cyclic voltammogram was observed (curve c), which may be due to the negatively charged AuNPs repelling the probe $[Fe(CN)_6]^{3-/4-}$. The reversibility and peak current of the probe obviously decrease after the capture probe DNA (S1) is immobilized on the AuNPs/ CuS-Gr/GCE (curve d), which is due to electrostatic repulsion between the negatively charged HS-ssDNA and $[Fe(CN)_6]^{3-/4-}$. The peak currents further decrease after the S1/AuNPs/ CuS-Gr/GCE hybridizes with the target DNA (S2) (curve e), which is attributed to the double-stranded DNA retarding the electron transfer.

Figure 4b shows the cyclic voltammograms of different electrodes, including the bare GCE, the AuNPs/GCE, the graphene/GCE, the CuS/GCE, and the CuS-Gr/GCE. It shows that the best reversibility and the smallest ΔE_p are obtained for the CuS-Gr/GCE. The presence of graphene or CuS on the GCE increases the peak currents owing to their good conductivity. Although the AuNPs do not increase the peak current of $[Fe(CN)_6]^{3-/4-}$, they obviously decrease ΔE_p and have a key role in immobilizing the HS-ssDNA. All these results indicate that the CuS-Gr composite is an effective base for sensitive electrochemical DNA biosensor construction.

Optimization of experimental conditions

The reaction time of probe HS-ssDNA covalently immobilized on the AuNPs/CuS-Gr/GCE by the Au–thiol chemistry affected the electrochemical response of the DNA sensor. The effect of reaction time on the DPV signal of $[Fe(CN)_6]^{3-/4-}$ is sown in Fig. 5a. It shows that the peak current of $[Fe(CN)_6]^{3-/4-}$ increases with the reaction time in the range from 3 to 12 h. The
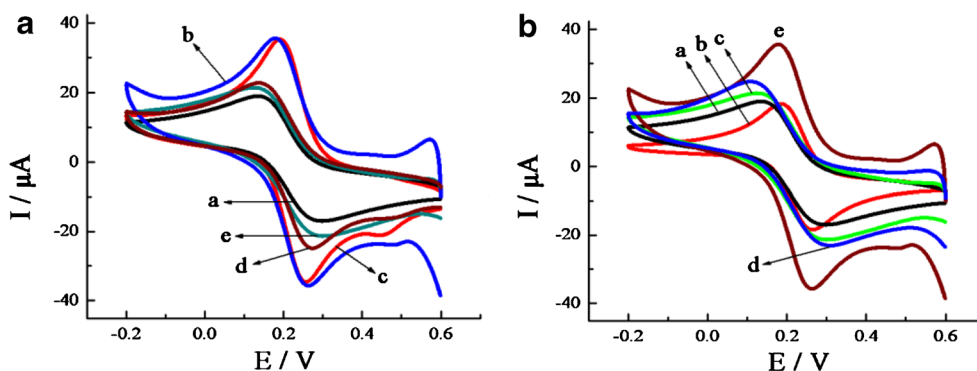
Fig. 4 a Cyclic voltammograms of the modified glassy carbon electrode (GCE) in 5 mM $[Fe(CN)_6]^{3-/4-}$ containing 0.1 M KCl: GCE (a), CuS-Gr/ GCE (b), AuNPs/CuS-Gr/GCE (c), S1/AuNPs/CuS-Gr/GCE (d), and S2– S1/AuNPs/CuS-Gr/GCE (e). b Cyclic voltammograms of the modified GCE in 5 mM $[Fe(CN)_6]^{3-/4-}$ containing 0.1 M KCl: GCE (a), AuNPs/ GCE (b), graphene/GCE (c), CuS/GCE (d), and CuS-Gr/GCE (e). See the text for an explanation of S1 and S2

Fig. 5 The effect of the reaction time of the AuNPs/CuS-Gr/GCE with S1 (**a**), hybridization time (**b**), and hybridization temperature of S1 with S2 (**c**) on the peak current
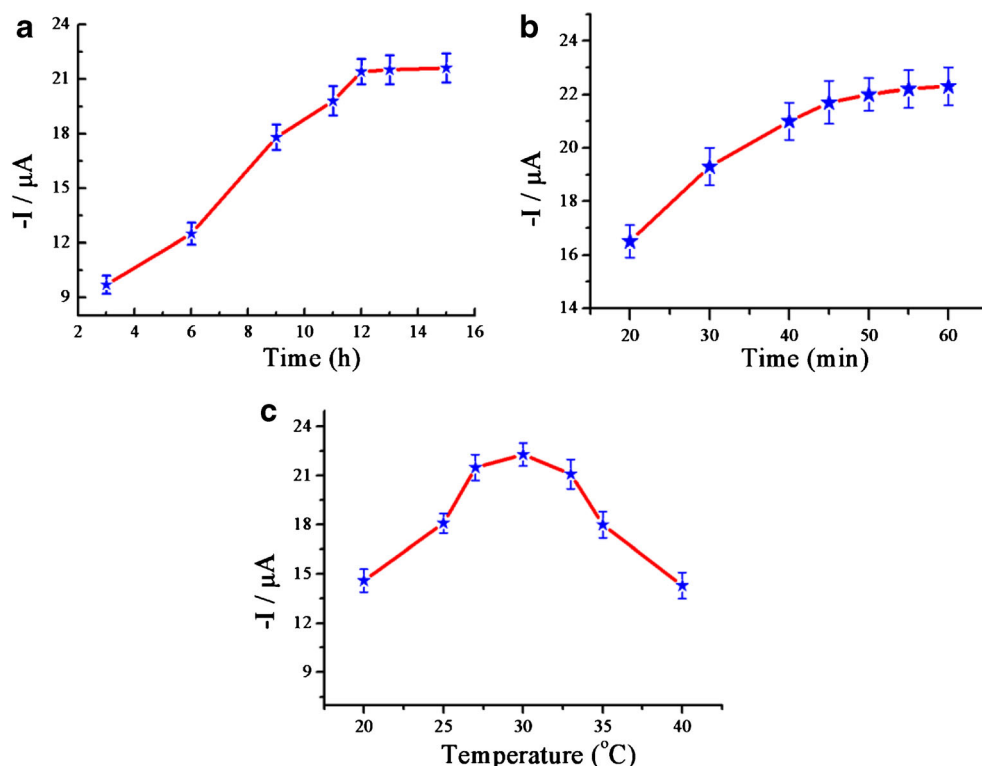

current response reaches a plateau after 12 h, indicating that most probe HS-ssDNA has been immobilized on the electrode. So the immobilization time of 12 h was used in further experiments.

The effect of time and temperature on the hybridization reaction between the capture probe DNA and the target DNA were also studied. Figure 5b shows the peak current of $[Fe(CN)_6]^{3-/4-}$ obviously increased with increase of the reaction time from 20 to 50 min, and remained almost stable after

50 min, suggesting that the hybridization reaction is complete. Thus, 50 min was applied for the hybridization time. Figure 5c shows the effect of the hybridization temperature on the peak current of $[Fe(CN)_6]^{3-/4-}$ in the range from 20 to 40 °C. The peak current increases with increase of temperature in the range from 20 to 30 °C and then decreases when the temperature increases further. Therefore, 30 °C was chosen as the hybridization temperature.
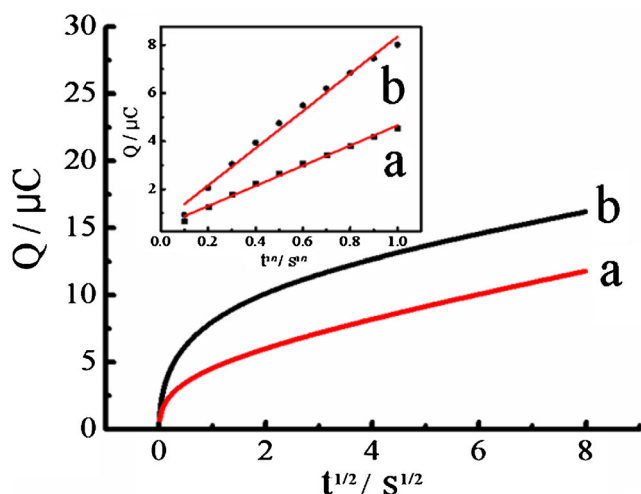
Fig. 6 Q–t curves of the bare GCE (*a*) and the AuNPs/CuS-Gr/GCE (*b*) in 0.1 mM $K_3[Fe(CN)_6]$ containing 1.0 M KCl. The *inset* shows Q–$t^{1/2}$ curves for the GCE (*a*) and the AuNPs/CuS-Gr/GCE (*b*)
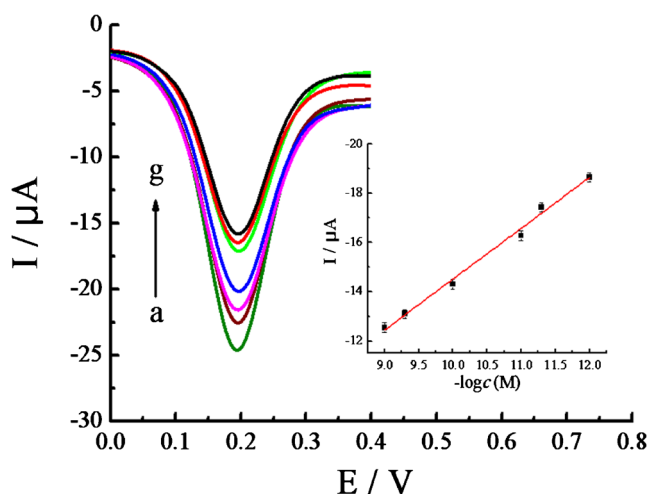
Fig. 7 Differential pulse voltammetry (DPV) curves of the DNA biosensor hybridized with increasing concentrations of complementary DNA: *from bottom to top* 1.0×10^{-12} M, 5.0×10^{-12} M, 1.0×10^{-11} M, 5.0×10^{-11} M, 1.0×10^{-10} M, 5.0×10^{-10} M, 1.0×10^{-9} M, and 1.0×10^{-8} M. The *inset* shows a logarithmic plot of the peak current versus the concentration of cDNA

Table 1 Comparison of different methods for DNA detection

Electrodes	Analytical technique	Linear range (nM)	LOD (pM)	Reference
$Ph-NH_2/GO/GCE$	EIS	0.001–100	0.11	[8]
Gr/polyaniline/GCE	DPV	0.0001–700	0.032	[25]
$CeO_2/SWNTs/BMIMPF_6/GCE$	EIS	0.001–100	0.23	[26]
$Chit/CeO_2/ZrO_2/Au$	DPV	0.000163–16.3	0.1	[27]
$CeO_2/Chit/GCE$	DPV	0.0159–116	10	[28]
4-ATP/AuNPs/Au	DPV	0.014–2	9.5	[7]
AuNPs/CuS-Gr/GCE	DPV	0.001–1	0.1	This work

4-ATP 4-aminothiophenol, *AuNPs* gold nanoparticles, *$BMIMPF_6$* 1-butyl-3-methylimidazolium hexafluorophosphate, *Chit* chitosan *DPV* differential pulse voltammetry, *EIS* electrochemical impedance spectroscopy, *GCE* glassy carbon electrode, *GO* graphene oxide, *Gr* graphene, *LOD* limit of detection, *Ph* phenylenediamine, *SWNTs* single-walled carbon nanotubes

Chronocoulometry

The effective surface areas of the bare GCE and the AuNPs/CuS-Gr/GCE were compared by chronocoulometry in 0.1 mM $K_3[Fe(CN)_6]$ containing 1.0 M KCl, where the standard diffusion coefficient (D_0) of $K_3[Fe(CN)_6]$ at 25 °C is 7.6×10^{-6} cm^2 s^{-1}. The effective surface area (A) of the electrodes was calculated according to the following equation:

$$Q = 2nFAcD^{1/2}t^{1/2}/\pi^{1/2} + Q_{dl} + Q_{ads}, \qquad (1)$$

where n is the number of electrons transferred, F (C mol^{-1}) is the Faraday constant, A (cm^2) is the area of the electrode, c (mol cm^{-3}) is the concentration of the substrate, D (cm^2 s^{-1}) is the diffusion coefficient, t is the time (s) Q_{dl} (C) is the double-layer charge, and Q_{ads} (C) is the adsorption charge. The values of A of the bare GCE and the AuNPs/CuS-Gr/GCE were calculated to be 0.045 cm^2 and 0.082 cm^2, respectively, according to the experimental results as shown in Fig. 6. The results suggested that the effective surface area of the electrode increased greatly after application of AuNPs/CuS-Gr composite film on the bare GCE

Determination of target DNA

Under the optimal experimental conditions, the differential pulse voltammograms for target DNA at different concentrations are shown in Fig. 7. The DPV response linearly increases with the logarithm of target DNA concentration (1.0 pM to 1 nM), and the corresponding regression equation was i_p (μA) $= 6.15 + 2.06 \times \lg C$ (M), with a correlation coefficient of 0.993. The detection limit is 0.1 pM, which is estimated as three times the standard deviation of the blank sample measurements. The different electrochemical biosensors for DNA determination are compared in Table 1. The proposed biosensor exhibited a much lower limit of detection [7, 8, 25–28]. The application of graphene and CuS in the DNA biosensor construction efficiently accelerated the electron transfer and enhanced the detection signal. Furthermore, AuNPs in the composite film increased the electrode surface area to support much more HS-ssDNA probe and thus lower the detection limit of the DNA target.

Selectivity

The selectivity of the present DNA biosensor was studied by reaction with different ssDNA sequences, including complementary target ssDNA sequences, one-base-mismatched ssDNA sequences, three-base-mismatched ssDNA sequences, and the noncomplementary target ssDNA sequence. Figure 8 shows the DPV signal of 1.0 nM $[Fe(CN)_6]^{3-/4-}$ at the different hybridized electrodes. The lowest current response is observed at the S2–S1/AuNPs/CuS-Gr/GCE (curve d), indicating the successful hybridization with more ssDNA on the electrode surface. The biggest response is shown at the
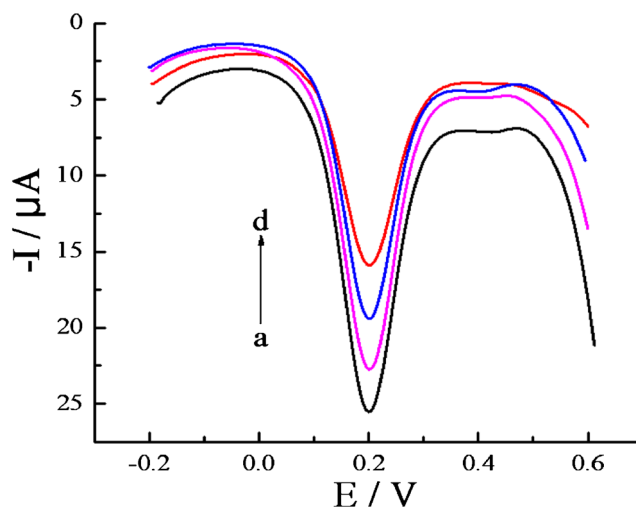
Fig. 8 DPV responses recorded after the biosensor had recognized the various DNA sequences: *from bottom to top* noncomplementary DNA, three-base-mismatched DNA, single-base-mismatched DNA, and cDNA

electrode when it is exposed to noncomplementary sequences (curve a), suggesting there are a few noncomplementary sequences on the electrode surface. The signals for one-base-mismatched and three-base-mismatched sequences (curves b and c) are significantly greater than that of the complementary sequences, indicating the hybridization is not achieved completely. These results demonstrate that the proposed biosensor had good selective recognition ability for complementary sequences, one-base-mismatched sequences, three-base-mismatched sequences, and the noncomplementary sequence.

Stability and reproducibility

The stability of the electrochemical DNA sensor was studied. The AuNPs/CuS-Gr/GCEs were placed in 0.1 M NaOH and 0.1 M HCl solutions at room temperature for 3 h, respectively, and no black suspension was observed, which indicated that the surface of the GCE was firmly coated with the AuNPs/CuS-Gr film.

Furthermore, the S1/AuNPs/CuS-Gr/GCEs were placed in water and PBS (pH 7.0) for 6 h. Then, the soaked electrodes were measured by DPV in 5.0 mM $[Fe(CN)_6]^{3-/4-}$ containing 0.1 M KCl. The current response obtained at the unincubated electrode was -21.1 μA. The current responses obtained at the electrodes incubated in water and PBS were -21.0 μA and -21.3 μA, respectively. Further, UV–vis experiments (monitoring the soaking solution after S1/AuNPs/CuS-Gr/GCEs had been dipped in it) showed that no characteristic UV absorption peak occurred at 260 nm for DNA. The results illustrate that the S1/AuNPs/CuS-Gr/GCE maintained good stability.

The reproducibility of the as-prepared DNA biosensor was also investigated. Six parallel-made S1/AuNPs/CuS-Gr/GCEs were applied to detect 5×10^{-11} M target DNA. The relative standard deviation of the biosensor was 4.7 %, indicating good reproducibility.

Conclusions

In this work, a novel CuS-Gr composite was synthesized by a hydrothermal method to achieve excellent electrochemical properties for application as a DNA electrochemical sensing platform. The introduction of CuS-Gr composite and AuNPs in the construction of the biosensor efficiently accelerated the electron transfer and enhanced the detection signal, which led to high sensitivity with a detection limit of 0.1 pM. The as-prepared DNA biosensor also exhibited excellent ability to discriminate against DNA sequences that contain base mismatches. Therefore, this work will be attractive for genetic target analysis in bioanalytical and clinic biomedical application.

References

1. Guo Y, Chen JH, Chen GN (2013) A label-free electrochemical biosensor for detection of HIV related gene based on interaction between DNA and protein. Sensors Actuators B 184:113–117
2. Radhakrishnan S, Sumathi C, Umar A, Kim SJ, Wilson J, Dharuman V (2013) Polypyrrole-poly(3,4-ethylenedioxythiophene)-Ag (PPy-PEDOT-Ag) nanocomposite films for label-free electrochemical DNA sensing. Biosens Bioelectron 47:133–140
3. Liu BX, Hu JP, Foord JS (2012) Electrochemical detection of DNA hybridization by a zirconia modified diamond electrode. Electrochem Commun 19:46–49
4. Yao W, Wang L, Wang HY, Zhang XL, Li L, Zhang N, Pan L, Xing NN (2013) An electrochemiluminescent DNA sensor based on nano-gold enhancement and ferrocene quenching. Biosens Bioelectron 40: 356–361
5. Qiu SY, Li XH, Xiong WM, Xie LD, Guo LH, Lin ZY, Qiu B, Chen GN (2013) A novel fluorescent sensor for mutational p53 DNA sequence detection based on click chemistry. Biosens Bioelectron 41:403–408
6. Huang KJ, Liu YJ, Wang HB, Wang YY, Liu YM (2014) Sub-femtomolar DNA detection based on layered molybdenum disulfide/multi-walled carbon nanotube composites, Au nanoparticle and enzyme multiple signal amplification. Biosens Bioelectron 55: 195–202
7. Li GJ, Liu LH, Qi XW, Guo YQ, Sun W, Li XL (2012) Development of a sensitive electrochemical DNA sensor by 4-aminothiophenol self-assembled on electrodeposited nanogold electrode coupled with Au nanoparticles labeled reporter ssDNA. Electrochim Acta 63:312–317
8. Hu YW, Li FH, Han DX, Wu TS, Zhang QX, Niu L, Bao Y (2012) Simple and label-free electrochemical assay for signal-on DNA hybridization directly at undecorated graphene oxide. Anal Chim Acta 753:82–89
9. Spain E, Keyes TE, Forster RJ (2013) DNA sensor based on vapour polymerised pedot films functionalised with gold nanoparticles. Biosens Bioelectron 41:65–70
10. Spain E, Keyes TE, Forster RJ (2013) Polypyrrole-gold nanoparticle composites for highly sensitive DNA detection. Electrochim Acta 109:102–109
11. Dong HF, Zhu Z, Ju HX, Yan F (2012) Triplex signal amplification for electrochemical DNA biosensing by coupling probe-gold nanoparticles-graphene modified electrode with enzyme functionalized carbon sphere as tracer. Biosens Bioelectron 33:228–232
12. Muti M, Kuralay F, Erdem A (2012) Single-walled carbon nanotubes-polymer modified graphite electrodes for DNA hybridization. Colloids Surf B 91:77–83
13. Yin Z, Sun S, Salim T, Wu S, Huang X, He Q, Lam YM, Zhang H (2010) Organic photovoltaic devices using highly flexible reduced graphene oxide films as transparent electrodes. ACS Nano 4: 5263–5268
14. Ghosh S, Sarker BK, Chunder A, Zhai L, Khondaker SI (2010) Position dependent photodetector from large area reduced graphene oxide thin films. Appl Phys Lett 96:163109–163109
15. Huang KJ, Wang L, Li J, Liu YM (2013) Electrochemical sensing based on layered MoS₂-graphene composites. Sensors Actuators B 178:671–677
16. Huang J, Zhang L, Chen B, Ji N, Chen F, Zhang Y, Zhang Z (2010) Nanocomposites of size-controlled gold nanoparticles and graphene

oxide: formation and applications in SERS and catalysis. Nanoscale 2:2733–2738

17. Jiao S, Xu L, Jiang K, Xu D (2006) Well-defined non-spherical copper sulfide mesocages with single-crystalline shells by shape-controlled Cu_2O crystal templating. Adv Mater 18:1174–1177

18. Janata J, Josowicz M, DeVaney DM (1994) Chemical sensors. Anal Chem 66:207R–228R

19. Zou J, Jiang J, Huang L, Jiang H, Huang K (2011) Synthesis, characterization and electrocatalytic activity of copper sulfide nanocrystals with different morphologies. Solid State Sci 13:1261–1267

20. Niu SY, Sun J, Nan CC, Lin JH (2013) Sensitive DNA biosensor improved by 1,10-phenanthroline cobalt complex as indicator based on the electrode modified by gold nanoparticles and graphene. Sensors Actuators B 176:58–63

21. Wilson J, Radhakrishnan S, Sumathi C, Dharuman V (2012) Polypyrrole-polyaniline-Au (PPy-PANi-Au) nano composite films for label-free electrochemical DNA sensing. Sensors Actuators B 171–172:216–222

22. Li L, Wang S, Yang T, Huang SM, Wang JC (2012) Electrochemical growth of gold nanoparticles on horizontally aligned carbon nanotubes: a new platform for ultrasensitive DNA sensing. Biosens Bioelectron 33:279–283

23. Hummers W, Offeman R (1958) Preparation of graphitic oxide. J Am Chem Soc 80:1339–1340

24. Tian Q, Tang M, Sun Y, Zou R, Chen Z, Zhu M, Yang S, Wang J, Wang J, Hu J (2011) Hydrophilic flower-like CuS superstructures as an efficient 980 nm laser-driven photothermal agent for ablation of cancer cells. Adv Mater 23:3542–3547

25. Du M, Yang T, Li X, Jiao K (2012) Fabrication of DNA/graphene/polyaniline nanocomplex for label-free voltammetric detection of DNA hybridization. Talanta 88:439–444

26. Zhang W, Yang T, Zhuang X, Guo Z, Jiao K (2009) An ionic liquid supported CeO_2 nanoshuttles-carbon nanotubes composite as a platform for impedance DNA hybridization sensing. Biosens Bioelectron 24:2417–2422

27. Wang QX, Gao F, Zhang X, Zhang B, Li SX, Hu ZS, Gao F (2012) Electrochemical characterization and DNA sensing application of a sphere-like CeO_2-ZrO_2 and chitosan nanocomposite formed on a gold electrode by one-step electrodeposition. Electrochim Acta 62:250–255

28. Feng KJ, Yang YH, Wang ZJ, Jiang JH, Shen GL, Yu RQ (2006) A nano-porous CeO_2/chitosan composite film as the immobilization matrix for colorectal cancer DNA sequence-selective electrochemical biosensor. Talanta 70:561–565